AD-A172 249 SONDRESTROM RADAR OBSERVATIONS OF THE EFFECT OF THE IMF 1/1
BY COMPONENT ON P (U) SRI INTERNATIONAL MENLO PARK CA
O DE LA BEAUJARDIERE ET AL 1985 AFOSR-TR-86-0533
UNCLASSIFIED F49620-83-K-0005 F/G 4/1 NL

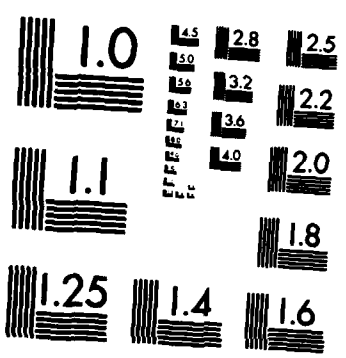

SONDRESTROM RADAR OBSERVATIONS OF THE EFFECT OF THE IMF B_y COMPONENT ON POLAR CAP CONVECTION

O. de la Beaujardière, V. B. Wickwar,
SRI International
Menlo Park, California 94025

J. H. King
NASA, National Space Science Data Center
Greenbelt, Maryland 20771

ABSTRACT

Average patterns of convection, derived from Sondrestrom radar observations, reveal that the interplanetary magnetic field dawn-dusk component (IMF B_y) strongly influences the nighttime polar convection. The convection for one orientation of B_y is not the mirror image of the other orientation. A positive B_y seems to organize the velocities such that, at all local times, they are predominantly westward within the radar latitude range. On a case-by-case basis, auroral oval boundaries can be determined by coincident DMSP particle data and by radar-measured E-region densities. On one occasion of positive B_y, sunward flow (i.e., westward flow) is observed in the polar cap between dusk and midnight. For large negative B_y, large southward velocities are observed about three hours before midnight. These are the only times when the predominant velocity component is clearly southward. When B_y is negative, in the midnight and dawn sectors, the plasma velocities appear random. However, the average drifts are mostly southward. The radar average patterns are compared with theoretical predictions and recently proposed convection patterns. Although none of the models seem to reproduce the observed convections well, some features present in the models are also seen in the radar data.

Introduction

There is little doubt that the interplanetary magnetic field strongly influences the magnetospheric and ionospheric convection [*Svalgaard*, 1968, 1973; *Mansurov*, 1969; *Friis-Christensen et al.*, 1985 and references therein]. However, the exact processes involved in the solar-wind/magnetosphere coupling are not well known, nor is the exact response of the large-scale convection. Our inability to measure an instantaneous snapshot of the global convection pattern has made it difficult to establish what electric field configuration corresponds to each IMF orientation. The range of possibilities is exemplified by the variety of convection patterns proposed in recent publications [*Potemra et al.*, 1984; *Reiff and Burch*, 1985; *Chiu et al.*, 1985; *Friis-Christensen et al.*, 1985]. The main focus of these papers was on the noon sector, because this is where the connection between the solar wind and the ionospheric plasma is the most direct [e.g., *Jorgensen et al.*, 1972, 1981; *Crooker*, 1979]. In contrast, the nightside of the polar convection has not been studied very extensively. However, early works by *Heppner* [1972, 1977] and *Mozer* [1974] indicate that the B_y component has an effect on the nightside convection as well.

The purpose of this paper is to examine the effect of the IMF B_y component in the dusk, midnight, and dawn sectors. Sondrestrom incoherent-scatter radar measurements of plasma drift in the auroral oval and the polar cap are used. In a previous paper [*de la*

To be published in Proceedings of the Chapman Conference on Solar Winds/Magnetosphere Coupling
Revised Version, July 18, 1985

Beaujardière et al., 1985a] the effect of the B_y component was derived from a case-by-case examination of the data. In this paper, we briefly review the individual radar observations and then show average convection patterns obtained by binning the drift data for the two orientations of the IMF B_y component. These patterns are compared to the various models of convection that have been proposed.

Ground-based observations of plasma convection have an advantage over space-borne observations in that they are continuous over long periods of time--several hours or days. Furthermore, the incoherent-scatter radars have an advantage over other ground-based instruments such as magnetometers in that they measure the ion velocity directly rather than infer it using mathematical inversion techniques that rely heavily on conductivities [*Kamide and Richmond*, 1982].

Observations

The radar data were obtained during 24-hr continuous observations. The operating mode for these runs is described in *Wickwar et al.* [1984]. Electric fields and profiles of ionospheric parameters were measured between 68° and 82° invariant latitude with a cycle time of about 20 minutes.

There is a total of 14 day-long experiments for which the IMF data are available from the IMP-J satellite. The data for four fairly typical days are shown in Figures 1 and 2. The IMF components in GSM coordinates are plotted on Figure 1, and the radar-measured plasma drifts are in Figure 2. The velocity vectors are color coded to show more clearly the regions of sunward or antisunward flow. The blue vectors are for eastward drifts, and the red vectors for westward drifts. The IMF vectors in the YZ plane are reproduced along the inside circle. Positive B_z point towards the center of the circle, and positive B_y towards the west direction (see Figure 2d). The vectors are red and blue for positive and negative B_y, respectively. DMSP particle data were used to show the position of the auroral oval [*Gussenhoven et al.*, 1983]. The oval boundaries were determined from coincident passes and are indicated by wide blue arrows (these arrows tend to disappear among the convection vectors; therefore, the times at which the satellite passes occurred are marked by a thinner arrow on the outside periphery).

These four examples show the characteristics in the convection patterns that have been seen in the other Sondrestrom 24-hr runs. Figure 2 is taken from *de la Beaujardière et al.* [1985a] where these observations are described in some detail. The available data were averaged and the results are shown in Figure 3a and 3b for B_y positive and negative, respectively. The data were averaged in bins of one degree by one hour. The drift components were weighted according to their statistical uncertainty. The selection was based on 10-min IMF averages, and the times considered were offset by 10 min to take into consideration the propagation times.

The conclusions reached on a case-by-case basis by *de la Beaujardière et al.* [1985a] are still valid when examining the averaged data. The main features of the convection pattern illustrated both by the four examples of Figure 2, and by Figure 3 can be briefly described as follows:

(1) *Case* $B_y > 0$.

When B_y is positive, the velocities are predominantly westward within the radar field of view at all local times (Figure 3a). Figure 2b offers a clear individual example: B_y remained positive throughout the observation period, and the radar appears to remain under a large westward vortex for 24 hours.

A shear convection reversal is observed in the morning cell. See, for example Figures 2b, 2c, and 3a.

The observations of 23-24 April are discussed by *de la Beaujardière et al.* [1985b] who show that between dusk and midnight on 23-24 April 1983, sunward (westward) flow is observed within the polar cap (Figure 2a). Following *Gussenhoven et al.* [1981], the auroral oval is taken as the region where the integral number flux and the energy flux rise noticeably above background. When considering Sondrestrom data alone, the oval is defined as the region where discernible E-region precipitation is observed (i.e., where the density is above $\sim 3 \times 10^4$ el/cm^3, in the absence of solar EUV production).

(2) *Case* $B_y < 0$.

In the midnight and dawn sectors, when B_y is negative, the plasma velocities are small and random in the individual observations (see 18 January, Figure 2d). The velocities also appear quite irregular in the midnight and dawn sector of the average pattern (Figure 3b) but, in the midnight

sector, the dominant averaged component is often southward. For large negative B_y, the afternoon cell appears shifted toward early hours such that large southward velocities are observed about 3 hours before midnight, as in the case of 24 July (Figure 2c). Large southward velocities are only observed in these premidnight hours, when B_y is large and negative.

A shear convection reversal is observed in the afternoon cell (Figure 2a, 2c, 2d, and 3c), symetrical to that seen in the morning cell when $B_y > 0$.

In conclusion, the nightside convection is strongly influenced by the B_y component. This influence is quite complex. The color convention for the IMF and drift vectors in Figure 2 reveals clearly that a "red" (positive) B_y corresponds to a "red" (westward) convection, and a "blue" (negative) B_y corresponds to a "blue" (eastward) velocity. In other words, in the poleward edge of the oval and in the polar cap, the drifts are mainly westward for positive B_y, and eastward for negative B_y. However, the convection for one orientation of B_y is not the mirror image of that of the other orientation.

Discussion

We now compare the radar observations with the various empirical models or schematic convection patterns that have been published. Examples of some recent models are shown in Figures 4, 5, and 6, in two columns, with positive B_y patterns on the left, and negative B_y on the right. The two pairs in Figure 4 are from *Potemra et al.* [1979] and *Maynard* [1985]. In these works, the B_z component was not taken into consideration. The patterns on Figures 5 and 6 are for negative and positive B_z, respectively. They are from *Reiff and Burch* [1985], *Friis-Christensen et al.* [1985], and *Potemra et al.* [1984].

The first impression one has when comparing the observations with these various models, is that in the nightside, none of the models match the observations well. A possible reason for this poor match is that most of these models are based on observations close to noon. Even the electrostatic potential configuration obtained by *Friis-Christensen et al.* [1985] (Figures 5 and 6, lowest panels), are mostly valid in the dayside, because the potential function derived from magnetograms depends greatly on the conductivity model adopted. On the dayside this model is know with reasonabl accurancy, but not on the nighside where the position & strengh of auroral precipitation are not well known. In the Heppner model shown by *Maynard* [1985], the dayside convection has been updated from the *Heppner* [1977] model with recent DE-2 data but not the nightside convection. These nightside patterns were based on Barium releases and on OGO-6 measurements. OGO-6 only yielded one component of the velocity, and, in addition, the OGO-6 noon-midnight passes suffered from spacecraft attitude problems [*Maynard*, 1974]. However, the Heppner and Friis-Christensen models, which are based in part on nightside observations, do not indicate that the pattern for one sign of B_y is symmetric to that for the opposite B_y. This behavior is in disagreement with all the other schematic patterns, but the Sondrestrom observations confirm this lack of symmetry. Interestingly, however, the radar observations seem to indicate that the influence of the B_y component is stronger than what is implied by Heppner's and Friis-Christensen's models.

When considering only the dawn or dusk local times, the simple Potemra patterns of Figure 4c and 4d correspond well to the observations. This is also apparent in the Sondrestrom data shown by *Robinson et al.* [1985]. A narrow convex cell with a sharp convection reversal is located on the afternoon side when B_y is negative, and on the morning side when B_y is positive. A similar topology was also observed by *Heelis et al.* [1983] using MITHRAS data.

The convection pattern is also dependent on B_z and, possibly, B_x, as well as season and substorm disturbances. In particular, to examine how the B_z component affects the average patterns, the radar observations were binned according to the sign of B_z as well as of B_y. The patterns appeared more noisy and the number of vectors in several bins were too small to allow conclusive determination of the dependence on B_z. However, these patterns appeared very similar to the averages shown in Figure 3. The main characteristics of the observations summarized above remain valid. The only noticeable difference was that the latitudes of the reversals were lower for negative B_z, as can be expected.

One difficulty in comparing the observations with the models is that the radar field of view can be either in the auroral oval, or in the polar cap, depending on the geomagnetic activity or,

equivalently, on the $-B_z$ component. It is to alleviate this difficulty that oval boundaries are indicated in Figure 2. However the definition of polar cap is highly dependent on the physical parameters that are measured and on the set of instruments used [*Torbert et al.*, 1981].

Sunward flow in the polar cap has been observed experimentally [*Maezawa*, 1976; *Heppner*, 1977; *Burke et al.*, 1979; *Burch et al.*, 1985], but most such observations were in the dayside of the polar cap. The Sondrestrom data seem to indicate that sunward (westward) flows can occur around magnetic midnight in the polar cap, where the polar cap is determined by the DMSP and radar observations.

Sunward drifts in the polar cap were also predicted theoretically by *Stern* [1973], *Lyons* [1985], *Reiff and Burch* [1985], and *Chiu et al.* [1985]. In these models, the flow in the polar cap is mostly clockwise for positive B_y, and counterclockwise for negative B_y. The Sondrestrom observations seem to be consistent with the former, but not the latter case.

The fact that the convection pattern appears disorderly when B_y is negative, may be explained in part by Lyons' model. The polar cap convection that he infers for $B_y < 0$ is very complex. Because the actual IMF components are not constant in time but vary continuously, this pattern is highly variable. As a result, as the various elements of this intricate pattern move around, the observed drifts appear disorderly.

The Potemra and Reiff patterns of Figures 5 and 6 show a complex cell topology. The fact that these multiple cells are not readily apparent in the radar data should not be taken as conclusive evidence that they do not exist. The radar latitude is often too low to see some of the reversals predicted in the polar cap. Also, as pointed out by *Burch et al.* [1985], the viscous cell (marked V in Figures 5 and 6) can be extremely narrow and, thus, could have been missed by the radar whose spatial resolution is about 100 km at the farthest latitudes.

Conclusion

In conclusion, these Sondrestrom observations reveal that the IMF B_y component strongly influences the nightside polar convection. Various models were compared with the radar observations. Although none of them offer a very good match, some features from each model are found in the observations:

- When $B_y > 0$, the velocities are predominantly westward, at all local times. This is in agreement with schematic diagrams [*Potemra et al.*, 1979, 1984; *Reiff and Burch*, 1985], and with theoretical predictions [*Stern*, 1973; *Lyons*, 1985; *Chiu et al.*, 1985].
- When $B_y < 0$, the convection is small and appears random. This is akin to Birkeland-current observations by *Zanetti et al.* [1984], and may be explained in part by *Lyons* [1985].
- There is a tendency to observe velocity shears in the morning (evening) convection cells for B_y positive (negative). This matches well the *Potemra et al.* [1979] sketch.
- In the nightside, the convection for one orientation of B_y is not symmetric to the pattern for the other orientation. This asymmetry is in disagreement with most schematic patterns proposed, but it is present in the empirical models of *Heppner* [1977] and *Friis-Christensen et al.* [1985].

Acknowledgments

This work was supported by NSF cooperative agreement ATM8121671 and AFOSR contract F49620-83-K-0005. Our thanks go to D. Hardy, S. Gussenhoven, and N. Heinnman who provided the DMSP data.

References

Burch, J. L., P. H. Reiff, J. D. Menietti, R. A. Heelis, W. B. Hanson, S. D. Shawhan, E. G. Shelley, M. Sugiura, D. R. Weimer, and J. D. Winningham, IMF B_y-dependent plasma flow and Birkeland currents in the dayside magnetosphere. 1. Dynamics Explorer observations, *J. Geophys. Res.*, *90*, 1577, 1985.

Burke, W. J., M. C. Kelley, R. C. Sagalyn, M. Smiddy, and S. T. Lai, Polar cap electric field structures with a northward interplanetary magnetic field, *Geophys. Res. Letts.*, *6*, 21, 1979.

Chiu, Y. T., N. U. Crooker. amd D. J. Gorney, Model of oval and polar cap arc configurations, *J. Geopys. Res.*, *90*, 5153, 1985.

Crooker, N. U., Dayside merging and cusp geometry, *J. Geophys. Res.*, *84*, 951, 1979.

de la Beaujardière, O., V. B. Wickwar, J. D. Kelly, and J. H. King, IMF-B_y effect on the high-latitude nightside convection, *Geophys. Res. Letts.*, *12*, 461, 1985a.

de la Beaujardière, O., V. B. Wickwar, and J. D. Kelly, Observations of polar-cap ionospheric signatures of solar wind/magnetosphere coupling, in *Results of THE ARCAD 3 PROJECT and of the recent programmes in magnetospheric and ionospheric physics, Toulouse 84*, 353, Cepadues-Editions, France, 1985b.

Friis-Christensen, E., Y. Kamide, A. D. Richmond, and S. Matsushita, Interplanetary magnetic field control of high-latitude electric fields and currents determined from Greenland magnetometer data, *J. Geophys. Res.*, *90*, 1325, 1985.

Gussenhoven, M. S., D. A. Hardy, and W. J. Burke, DMSP/F2 electron observations of equatorward auroral boundaries and their relationship to magnetospheric electric fields, *J. Geophys. Res.*, *86*, 768, 1981.

Gussenhoven, M. S., D. A. Hardy, and N. Heinemann, Systematics of the equatorward diffuse auroral boundary, *J. Geophys. Res.*, *88*, 5692, 1983.

Heelis, R. A., J. C. Foster, O. de la Beaujardière, and J. Holt, Multistation measurements of high-latitude ionospheric convection, *J. Geophys. Res.*, *88*, 10111, 1983.

Heppner, J. P., Polar-cap electric field distributions related to the interplanetary magnetic field direction, *J. Geophys. Res.*, *77*, 4877, 1972.

Heppner, J. P., Empirical models of high-latitude electric fields, *J. Geophys. Res.*, *82*, 1115, 1977.

Jorgensen, T. S., E. Friis-Christensen, and J. Wilhelm, Interplanetary magnetic field direction and high-latitude ionospheric currents, *J. Geophys. Res.*, *77*, 1976, 1972.

Jorgensen, T. S., Electric fields in the dayside auroral region, in *Exploration of the Polar Upper Atmosphere*, C. S. Deehr and J. A. Holtet (eds.), pp. 267, D. Reidel Publishing Company, Boston, Mass., 1981.

Kamide, Y., and A. D. Richmond, Ionospheric conductivity dependence of electric fields and currents estimated from ground magnetic observations, *J. Geophys. Res.*, *87*, 8331, 1982.

Lyons, L. R., A simple model for polar cap convection patterns and generation of [ESC 6 not implemented][ESC 6 not implemented]auroras, *J. Geophys. Res.*, *90*, 1561, 1985.

Maezawa, K., Magnetospheric convection induced by the positive and negative Z components of the interplanetary field: Quantitative analysis using polar cap magnetic records, *J. Geophys. Res.*, *81*, 2289, 1976.

Mansurov, S. M., New evidence of a relationship between magnetic fields in space and on Earth, *Geomagn. Aeron.*, Engl Transl., *9*, 662, 1969.

Maynard, N. C., Electric field measurements across the Harang discontinuity, *J. Geophys. Res.*, *79*, 4620, 1974.

Maynard, N. C., Structure in the DC and AC electric fields associated with the dayside cusp region, in *The Polar Cusp*, J. A. Holtet and A. Egeland (eds.), pp. 305-322, D. Reidel Publishing Company, 1985.

Mozer, F. S., W. D. Gonzalez, F. Bogott, M. C. Kelley, and S. Schutz, High-latitude electric fields and the three-dimensional interaction between the interplanetary and terrestrial magnetic fields, *J. Geophys. Res.*, *70*, 56, 1974.

Potemra, T. A., T. Iijima, and N. A. Saflekos, Large-scale characteristics of Birkeland currents, in *Dynamics of the Magnetosphere*, p. 165, D. Reidel, Hingham, Mass., 1979.

Potemra, T. A., L. J. Zanetti, P. F. Bythrow, and A. T. Y. Lui, B_y- dependent convection patterns during northward interplanetary magnetic field, *J. Geophys. Res.*, *89*, 9753, 1984.

Reiff, P. H., and J. L. Burch, IMF B_y-dependent plasma flow and Birkeland currents in the dayside magnetosphere: 2. A global model for northward and southward IMF, *J. Geophys. Res.*, *90*, 1595, 1985.

Robinson, R. M., C. R. Clauer, O. de la Beaujardière, J. D. Kelly, and D. S. Evans, IMF B_y control of ionization and electric fields measured by the Sondrestrom radar, (this issue), *Proceedings of the Chapman Conference on Solar Wind/Magnetosphere Interactions*, 1985.

Stern, D. P., A study of the electric field in an open magneto- spheric model, *J. Geophys. Res.*, *78*, 7292, 1973.

Svalgaard, L., Sector structure of the interplanetary magnetic field and daily variation of geomagnetic field at high latitudes, *Geophys. Pap. R-6*, Dan. Meteorol. Inst., Copenhagen, Denmark, 1968.

Torbert, R. B., C. A. Cattell, F. S. Mozer, and C.-I. Meng, The boundary of the polar cap and its relation to electric fields, field-aligned currents, and auroral particle precipitation, *Physics of Auroral Arc Formation*, p. 143, S.-I. Akasofu and J. R. Kan (eds.), American Geophysical Union, Washington, D. C, 1981.

Wickwar, V. B., J. D. Kelly, O. de la Beaujardière, C. A. Leger, F. Steenstrup, and C. H. Dawson, Sondrestrom overview, *Geophys. Res. Lett.*, *11*, 883, 1984.

Zanetti, L. J., T. A. Potemra, T. Iijima, W. Baumjohann, and P. F. Bythrow, Ionospheric and Birkeland current distributions for northward interplanetary magnetic field: Inferred polar convection, *J. Geophys. Res.*, *89*, 7453, 1984.

Figure Captions

Fig. 1. IMF parameters (GSM coordinates) from the IMP-J spacecraft for the four periods of Figure 2.

Fig. 2. Plasma drift and IMF B_y and B_z vectors for four typical examples. Red (blue) is for west (east) velocity, and for positive (negative) B_y. The thick blue arrows indicate the poleward or equatorward boundaries of the auroral oval, as determined from coincident DMSP passes.

Fig. 3. Average of ion drifts measured by the Sondrestrom radar, for B_y positive and negative.

Fig. 4. Convection patterns for the two orientations of B_y, derived independently of B_z.

Fig. 5. Convection patterns for B_z negative.

Fig. 6. Convection patterns for B_z positive.

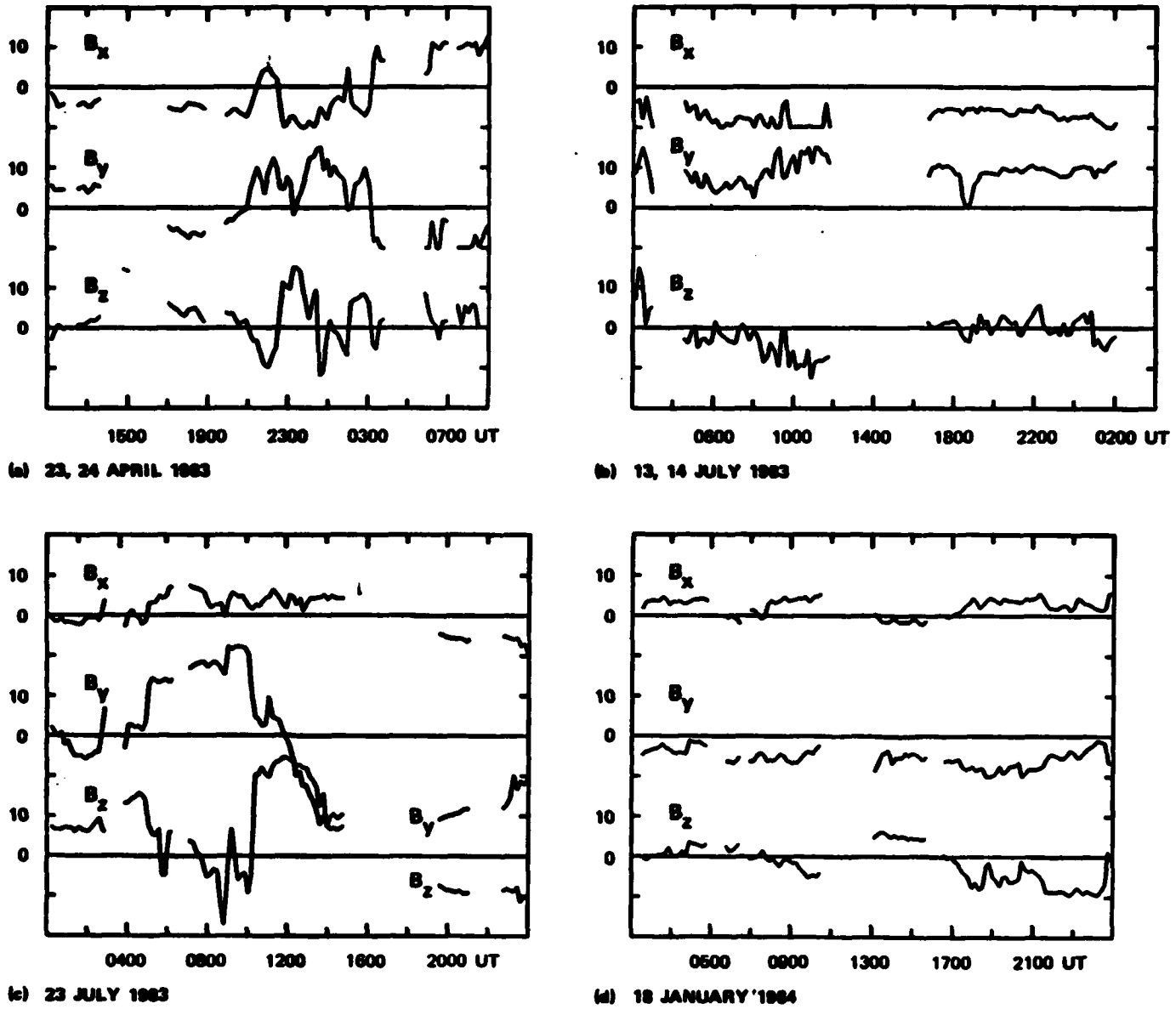

Fig. 1. IMF parameters (GSM coordinates) from the IMP-J spacecraft for the four periods of Figure 2.

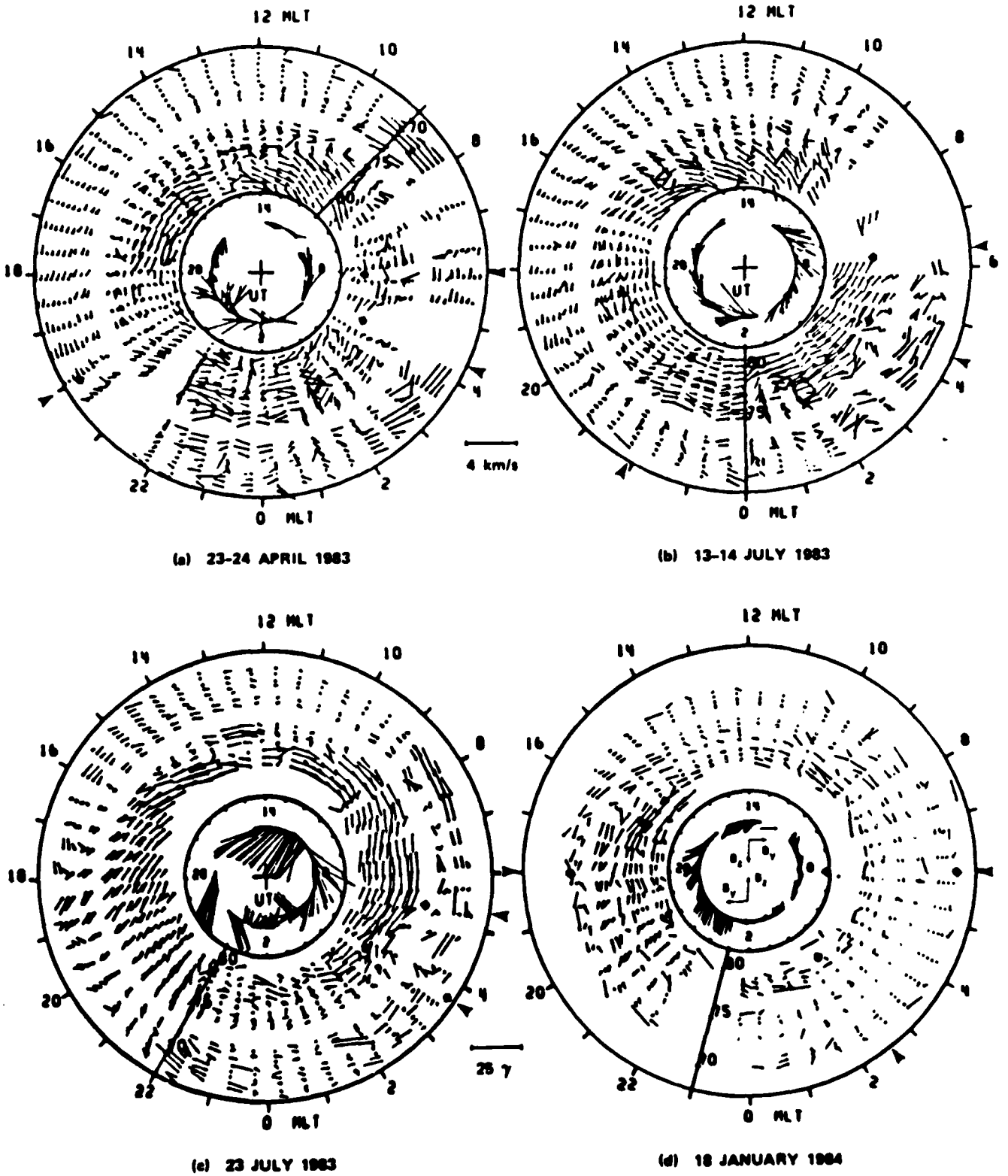

Fig. 2. Plasma drift and IMF B_y and B_z vectors for four typical examples. Red (blue) is for west (ea velocity, and for positive (negative) B_y. The thick blue arrows indicate the poleward equatorward boundaries of the auroral oval, as determined from coincident DMSP passes.

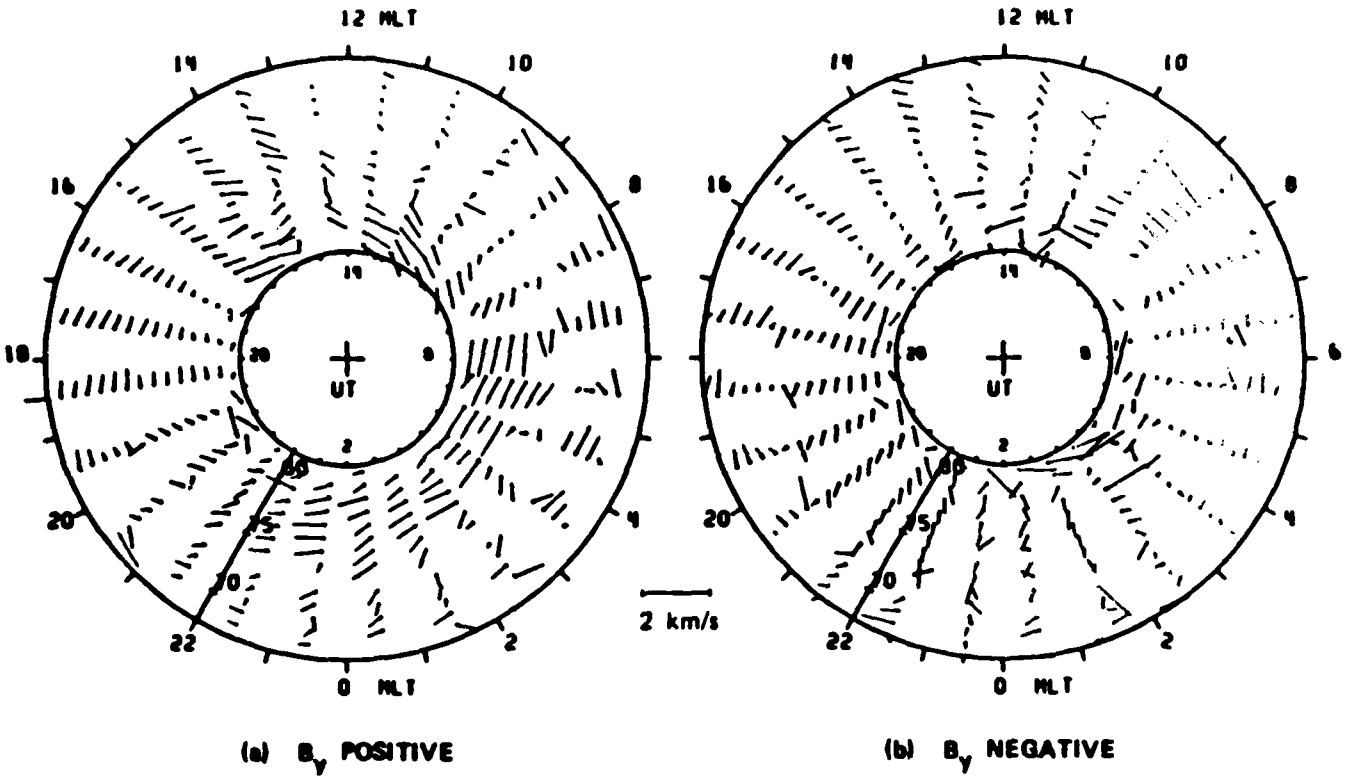

Fig. 3 Average of ion drifts measured by the Sondrestrom radar, for B_y positive and negative.

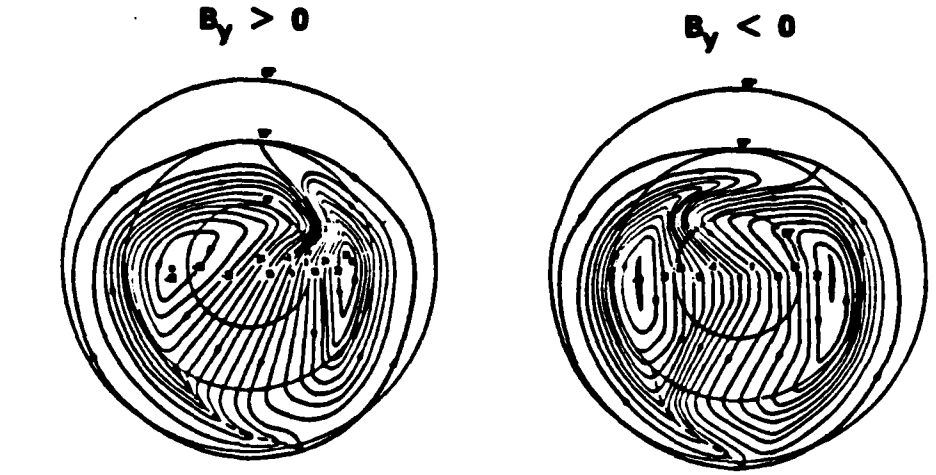

[Source: Heppner, 1984]

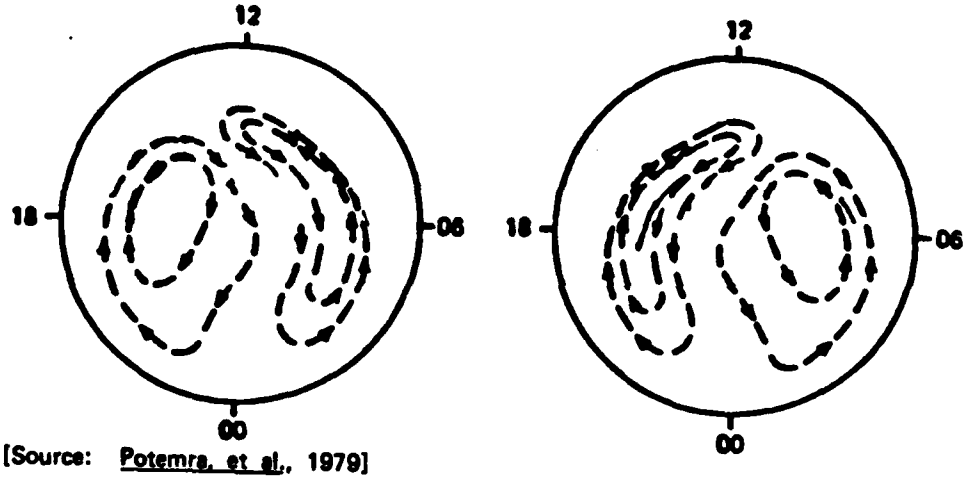

[Source: Potemra, et al., 1979]

Fig. 4. Convection patterns for the two orientations of B_y, derived independently of B_z.

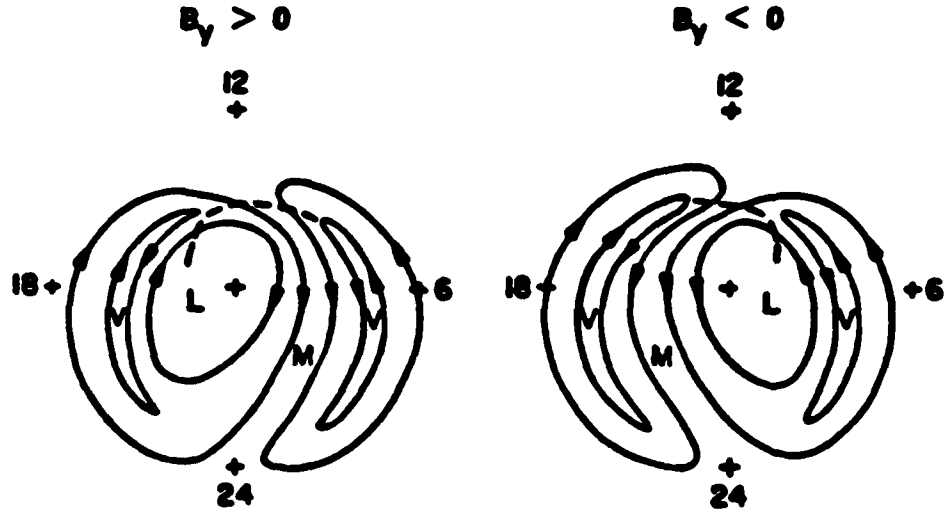

[Source: Reiff and Burch, 1985]

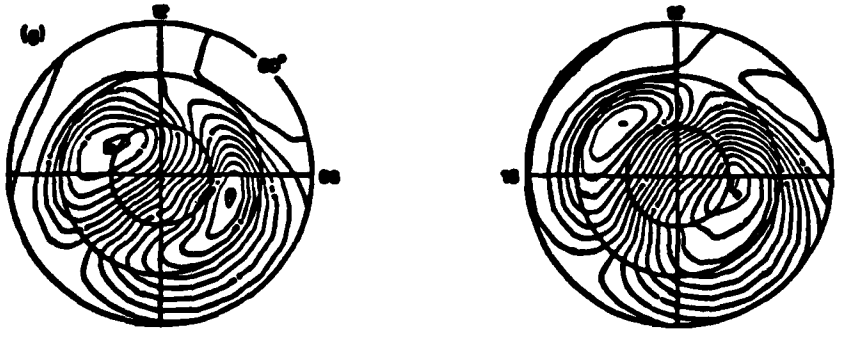

[Source: Friis-Christensen, et al., 1985]

Fig. 5. Convection patterns for B_z negative.

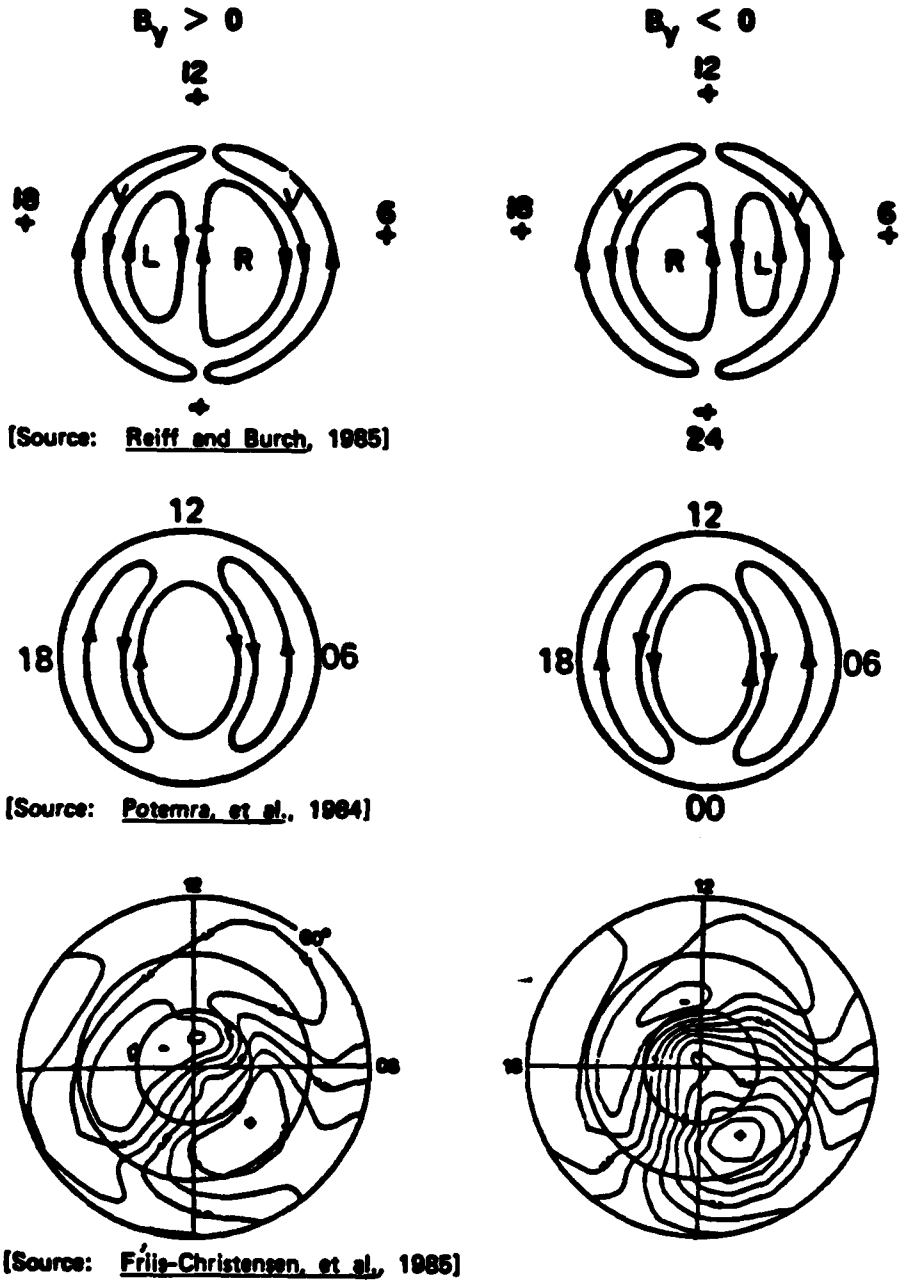

Fig. 6. Convection patterns for B_z positive.

REPORT DOCUMENTATION PAGE

1a. REPORT SECURITY CLASSIFICATION: Unclassified	1b. RESTRICTIVE MARKINGS
2a. SECURITY CLASSIFICATION AUTHORITY	3. DISTRIBUTION/AVAILABILITY OF REPORT: Approved for public release: Distribution unlimited
2b. DECLASSIFICATION/DOWNGRADING SCHEDULE	
4. PERFORMING ORGANIZATION REPORT NUMBER(S)	5. MONITORING ORGANIZATION REPORT NUMBER(S): AFOSR-TR- 86-0533
6a. NAME OF PERFORMING ORGANIZATION: SRI International; 6b. OFFICE SYMBOL (If applicable)	7a. NAME OF MONITORING ORGANIZATION: AFOSR/NC
6c. ADDRESS (City, State and ZIP Code): 333 Ravenswood Avenue, Menlo Park, CA 94025	7b. ADDRESS (City, State and ZIP Code): Bldg. 410, Bolling AFB D.C. 20332
8a. NAME OF FUNDING/SPONSORING ORGANIZATION: AFOSR; 8b. OFFICE SYMBOL (If applicable): NC	9. PROCUREMENT INSTRUMENT IDENTIFICATION NUMBER: F49620-83-K-0005
8c. ADDRESS (City, State and ZIP Code): Bldg. 410, Bolling AFB 20332	10. SOURCE OF FUNDING NOS.

PROGRAM ELEMENT NO.	PROJECT NO.	TASK NO.	WORK UNIT NO.
61102F	2310	A2	

11. TITLE (Include Security Classification): (See Title page) Sondrestrom Radar Observations of the Effect IMF By Component on Polar Cap Convection

12. PERSONAL AUTHOR(S): de la Beaujardiere, Wickwar, and King

13a. TYPE OF REPORT	13b. TIME COVERED	14. DATE OF REPORT (Yr., Mo., Day)	15. PAGE COUNT
reprint	FROM _____ TO _____		13

16. SUPPLEMENTARY NOTATION: To be published in Proceedings of the Chapman Conference on Solar Winds/Magnetosphere Coupling

17. COSATI CODES			18. SUBJECT TERMS (Continue on reverse if necessary and identify by block number)
FIELD	GROUP	SUB. GR.	Incoherent-scatter, ionosphere, magnetosphere, electric fields, auroral zone, interplanetary magnetic field

19. ABSTRACT (Continue on reverse if necessary and identify by block number)

Average patterns of convection, derived from Sondrestrom radar observations, reveal that the interplanetary magnetic field dawn-dusk component (IMF By) strongly influences the nighttime polar convection. The convection for one orientation of By is not the mirror image of the other orientation. A positive By seemsto organize the velocities such that, at all local times, they are predominantly westward within the radar latitude range. On a case-by-case basis, auroral oval boundaries can be determined by coincident DMSP particle data and by radar-measured E-region densities. On one occasion of positive By, sunward flow (i.e., westward flow) is observed in the polar cap between dusk and midnight. For large negative By, large southward velocities are observed about three hours before midnight. These are the only times when the predominant velocity component is clearly southward. When By is negative, in the midnight and dawn sectors, the plasma velocities appear random. However, the average drifts are mostly southward. The radar average patterns are compared with theoretical predictions and recently proposed convec-

20. DISTRIBUTION/AVAILABILITY OF ABSTRACT: UNCLASSIFIED/UNLIMITED ☒ SAME AS RPT. ☒ DTIC USERS ☐	21. ABSTRACT SECURITY CLASSIFICATION: Unclassified

22a. NAME OF RESPONSIBLE INDIVIDUAL	22b. TELEPHONE NUMBER (Include Area Code)	22c. OFFICE SYMBOL
Odile de la Beaujardiere	(415) 859-2093	

END

10-86

DTIC